0026-895X/11/7902-270–278$20.00
MOLECULAR PHARMACOLOGY
Vol. 79, No. 2
69054/3662471
Mol Pharmacol 79:270–278, 2011
Printed in U.S.A.

Differential Signaling of Cysteinyl Leukotrienes and a Novel Cysteinyl Leukotriene Receptor 2 ($CysLT_2$) Agonist, *N*-Methyl-Leukotriene C_4, in Calcium Reporter and β Arrestin Assays[S]

Dong Yan, Rino Stocco, Nicole Sawyer, Michael E. Nesheim, Mark Abramovitz,[1] and Colin D. Funk

Departments of Biochemistry (D.Y., M.E.N., C.D.F.) and Physiology (C.D.F.), Queen's University, Kingston, Ontario, Canada; and Department of Biochemistry and Molecular Biology, Merck Frosst Canada and Co., Pointe Claire-Dorval, Quebec, Canada (R.S., N.S., M.A.)

Received September 24, 2010; accepted November 15, 2010

ABSTRACT

The cysteinyl leukotrienes (cysLTs) LTC_4, LTD_4, and LTE_4 are lipid mediators with physiological and pathophysiological functions. They exert their effects through G protein-coupled receptors (GPCRs), most notably via $CysLT_1$ and $CysLT_2$ receptor. The roles of the $CysLT_2$ receptor are beginning to emerge. Both LTC_4 and LTD_4 are potent agonists for the $CysLT_2$ receptor; however, LTC_4 is rapidly converted to LTD_4, which is also the main endogenous ligand for the $CysLT_1$ receptor. A selective and potent agonist at the $CysLT_2$ receptor would facilitate studies to discern between receptor subtypes. We show here that *N*-methyl LTC_4 ($NMLTC_4$), a metabolically stable LTC_4 mimetic, is a potent and selective $CysLT_2$ receptor agonist. Two expression systems were used to evaluate the functional activity of $NMLTC_4$ at human and/or mouse $CysLT_1$ and $CysLT_2$ receptors. Through the aequorin cell-based assay for calcium-coupled GPCRs, $NMLTC_4$ was almost equipotent to LTC_4 at $CysLT_2$ receptors but was the least efficacious at $CysLT_1$ receptors. In a β-galactosidase–β-arrestin complementation assay, the human (h) $CysLT_2$ receptor can couple with β-arrestin-2, and $NMLTC_4$ is slightly more potent for eliciting β-arrestin-2 binding compared with cysLTs. Furthermore, LTE_4 is nearly inactive in this assay compared with its weak partial agonist activity in the aequorin system. In a vascular leakage assay, $NMLTC_4$ is potent and active in mice overexpressing $hCysLT_2$ receptor in endothelium, whereas the response is abrogated in $CysLT_2$ receptor knockout mice. Therefore, $NMLTC_4$ is a potent subtype selective agonist for the $CysLT_2$ receptor in vitro and in vivo, and it will be useful to elucidate its biological roles.

Introduction

Discovered as a bronchial constrictive agent, "slow-reacting substance of anaphylaxis" was later determined to represent a mixture of cysteinyl leukotrienes (cysLTs). Specifically, cysLTs are downstream metabolites of arachidonic acid derived from the 5-lipoxygenase product leukotriene A_4, conjugation of which with reduced glutathione gives rise to the first of the three cysLTs, LTC_4, by means of LTC_4 synthase (Funk, 2001). LTC_4 is exported from the cell by the multidrug resistance-associated protein-1 and sequential removal of the γ-glutamic acid moiety, by γ-glutamyl transpeptidase, and then the glycine residue, by aminopeptidases, gives rise to LTD_4 and LTE_4, respectively. CysLTs potentially exert their biological functions through five different GPCRs identified as $CysLT_1$, $CysLT_2$, GPR17, $CysLT_E$, and P2Y12 receptor.

Among these receptors, the $CysLT_1$ receptor is by far the most widely characterized, with expression observed in bronchial smooth muscle cells, spleen, leukocytes, and lung macrophages. LTD_4 is the preferred endogenous ligand for

This work was supported by the Canadian Institutes of Health Research [Grant MOP-68930]; the Canada Research Chairs program; and the Heart and Stroke Foundation of Ontario [Career Investigator award (to C.D.F.)].

[1] Current affiliation: Departments of Pathology and Oncology, Jewish General Hospital and Segal Cancer Centre, Montreal, Quebec, Canada.

Article, publication date, and citation information can be found at http://molpharm.aspetjournals.org.
doi:10.1124/mol.110.069054.

[S] The online version of this article (available at http://molpharm.aspetjournals.org) contains supplemental material.

ABBREVIATIONS: cysLT, cysteinyl leukotriene; Bay-u9773, 4-[[(1*R*,2*E*,4*E*,6*Z*,9*Z*)-1-[(1*S*)-4-carboxy-1-hydroxybutyl]-2,4,6,9-pentadecatetraenyl] thio]-benzoic acid; HAMI3379, 3-(((3-carboxycyclohexyl)amino)carbonyl)-4-(3-(4-(4-(cyclohexyloxy)butoxy)phenyl)propoxy)benzoic acid; $NMLTC_4$, *N*-methyl LTC_4; HA, hemagglutinin; α^*, N-terminal β-galactosidase fragment with H31R substitution; HEK, human embryonic kidney; DMEM, Dulbecco's modified Eagle's medium; FBS, fetal bovine serum; IRES, internal ribosomal entry site; GPCR, G protein-coupled receptor; PBS, phosphate-buffered saline; YFP, yellow fluorescent protein; PCR, polymerase chain reaction; ICI 204219, zafirlukast; MK679, *R*(−)-3-((3-(2-(7-chloro-2-quinolinyl)ethenyl) phenyl)(3-(dimethylamino)-3-oxo-propyl)thio)methyl)thio)propanoic acid; TG-EC, transgenic mice overexpressing the $hCysLT_2$ receptor in vascular endothelial cells; KO, knockout.

CysLT$_1$ receptor, and receptor activation elicits elevation in intracellular calcium levels (Lynch et al., 1999; Sarau et al., 1999). CysLT$_1$ receptor is the molecular target of the anti-asthmatic drugs montelukast (Singulair; Merck, Whitehouse Station, NJ), zafirlukast (Accolate; AstraZeneca Pharmaceuticals LP, Wilmington, DE) and pranlukast (Onon; Ono Pharmaceuticals, Osaka, Japan), which show efficacy in blocking inflammatory actions in the airways and improving airway function (Grossman et al., 1997; Suissa et al., 1997; Reiss et al., 1998).

The CysLT$_2$ receptor, on the other hand, has been less well characterized. Early pharmacological studies were compatible with CysLT$_2$ receptor expression in guinea pig trachea and ileum (Pong and DeHaven, 1983), ferret trachea and spleen (Aharony et al., 1985), in sheep bronchus, and in human pulmonary and saphenous vein preparations (Labat et al., 1992; Coleman et al., 1995; Walch et al., 1999). Molecular cloning of CysLT$_2$ receptor subsequently revealed expression in the heart, adrenal glands, placenta, and brain (Heise et al., 2000; Nothacker et al., 2000; Takasaki et al., 2000; Hui et al., 2001); more recently, CysLT$_2$ receptor was found to be selectively expressed in the vasculature of various organs and found to regulate vascular permeability (Moos et al., 2008). Various assays have shown that CysLT$_2$ receptor has a rank order potency of $LTC_4 = LTD_4 \gg LTE_4$, LTE_4 behaving as a partial agonist at both CysLT$_1$ and CysLT$_2$ receptors. LTE_4 acts as the preferred agonist for the CysLT$_E$ receptor (Maekawa et al., 2008), which has not yet been molecularly characterized. Until recently, the pharmacological inhibitor for CysLT$_2$ receptor has been the nonselective dual antagonist/partial agonist 4-[[(1*R*,2*E*,4*E*,6*Z*,9*Z*)-1-[(1*S*)-4-carboxy-1-hydroxybutyl]-2,4,6,9-pentadecatetraenyl]thio]-benzoic acid (Bay-u9773). However, Wunder et al. (2010) recently described the first selective CysLT$_2$ receptor antagonist, 3-(((3-carboxycyclohexyl)amino)carbonyl)-4-(3-(4-(4-(cyclohexyloxy)butoxy)phenyl)propoxy)benzoic acid (HAMI3379).

Here, we describe *N*-methyl LTC_4 ($NMLTC_4$), as the first selective agonist for CysLT$_2$ receptor, which, together with HAMI3379, should yield new insights into CysLT$_2$ receptor function. Moreover, using distinct functional assays, we reveal that, besides Ca^{2+} activation, the CysLT$_2$ receptor can interact with β-arrestin-2.

Materials and Methods

Materials. $NMLTC_4$ was synthesized initially as described previously (Gareau et al., 1993) and subsequently was obtained from Cayman Chemical Co. (Ann Arbor, MI). All cysLTs were also obtained from Cayman. Nucleotides ATP, ADP, UTP, and UDP were from Sigma-Aldrich (St. Louis, MO).

Aequorin Luminescence Assay. The following CysLT receptor constructs were used: for the mouse CysLT$_1$ receptor, the short-FLAG-mCysLT$_1$R-pcDNA3 that contains the influenza hemagglutinin signal sequence (HA) just upstream of the FLAG epitope, as described previously (Martin et al., 2001); for the human CysLT$_1$ receptor, the cDNA (Lynch et al., 1999) was subcloned into the short-FLAG-mCysLT$_1$R-pcDNA3 from which the cDNA for the mouse CysLT$_1$ receptor had been removed, resulting in construction of the HA-FLAG-hCysLT$_1$R-pcDNA3; for the mouse CysLT$_2$ receptor, pcDNA3-mCysLT$_2$R, as described previously (Hui et al., 2001); for the human CysLT$_2$ receptor, hCysLT$_2$R-pCR3.1, as described previously (Heise et al., 2000). The AEQ-pCDM plasmid (Molecular Probes, Carlsbad, CA) was used to express aequorin in the HEK 293 cells.

Human embryonic kidney (HEK) 293 cells stably expressing the simian vacuolating virus 40 large T antigen or HEK 293 cells stably expressing the Epstein-Barr virus nuclear antigen were grown in Dulbecco's modified Eagle's medium (DMEM) supplemented with 10% heat inactivated fetal bovine serum, 1 mM sodium pyruvate, 100 U/ml penicillin-G, 100 μg/ml streptomycin sulfate, and 250 μg/ml active G418 (Geneticin) at 37°C in a humidified atmosphere of 6% CO_2 in air.

HEK 293 cells stably expressing either the simian vacuolating virus 40 large T antigen or the Epstein-Barr virus nuclear antigen were cotransfected with hCysLT$_2$R-pCR3.1, pcDNA3-mCysLT$_2$R, HA-FLAG-hCysLT$_1$R-pcDNA3, or short-FLAG-mCysLT$_1$R-pcDNA3 and AEQ-pCDM plasmids (5 μg of each DNA per 75-cm^2 culture flask), using the LipofectAMINE PLUS reagent (Invitrogen) according to the manufacturer's instructions. Cells were subsequently prepared for use in the aequorin luminescence functional assay as described previously (Ungrin et al., 1999). In brief, holo-aequorin was reconstituted in intact cells by charging 85%-confluent cultures for 1 h at 37°C in Ham's F12 medium [with 0.1% fetal bovine serum (FBS) and 25 mM HEPES at pH 7.3] (GIBCO BRL, Mississauga, ON, Canada) containing 30 μM reduced glutathione (Sigma-Aldrich) and 8 μM coelenterazine cp (Invitrogen, Burlington, ON, Canada). After charging, the cells were washed from the growth surface by pipetting up and down, rinsed once, and resuspended in Ham's F12 medium (modified as above) at 2 to 5 × 10^5 cells/ml. Experiments were performed using a Luminoskan RS plate reading luminometer (Thermo Fisher Scientific, Walham, MA). Leukotrienes, in ethanol, were serially diluted, in duplicate, in a white 96-well cliniplate FB (Thermo Fisher Scientific) using a Biomek (Beckman Coulter, Fullerton, CA) in a final volume of 100 μl in PBS (with 1.26 mM $CaCl_2$) so that the final solvent concentration was ≤2%. The plate was then loaded into the luminometer, and wells were tested sequentially starting at position A1, by rows. Cells were injected into the well, and light emission was recorded over 30 s (peak 1). The cells were then lysed by injection of 25 μl of 0.9% Triton X-100 solution in H_2O, and light emission was measured for an additional 10 s (peak 2). Fractional luminescence for each well was determined by dividing the area under peak 1 by the total area under peaks 1 and 2 (P1/(P1+P2)). These calculations were performed using the Lskan controller program, custom software written in LabView (National Instruments, Austin, TX). A Microsoft Excel-compatible data file was generated containing the raw traces, the calculated results for each well (P1, P2, P1+P2, and P1/(P1+P2)) and the drug concentrations. This data file was subsequently analyzed using the LDAM software in Excel, employing a modified version of the Levenberg-Marquardt four-parameter curve-fitting algorithm to calculate EC_{50} values.

Generation and Characterization of Cells for β-Galactosidase–β-Arrestin Complementation Assay. Retroviral constructs (pMFG-YFP-H31Rα*-IRES-CD8 and pWZL-βArrestin2-ω-IRES-Hygro) were generous gifts from Dr. Helen Blau (Stanford University, Stanford, CA). pMFG vector was previously engineered to include YFP-α* linked with an IRES-CD8 cassette. The α* fragment encodes the N terminus of β-galactosidase with a point mutation H31R, to decrease affinity between α- and ω-fragments of β-galactosidase. To insert the hCysLT$_2$ receptor sequence into pMFG, EcoRI and XhoI restriction sites (underlined) were added to the flanking regions by polymerase chain reaction (PCR) with Phusion DNA polymerase (Finnzymes, Espoo, Finland) using oligonucleotide primers: forward, 5′-TAGAATTCGCCATGGAGAGAAAATTTATGTCCTTG-3′; reverse, 5′-TACTCGAGTACTC TTGTTTCCTTTCTCAACC-3′ and hCysLT$_2$R template (Hui et al., 2001) and cloned into the MfeI-XhoI site to generate pMFG-hCysLT$_2$R-YFP-H31Rα*-IRES-CD8 (pMFG-hCysLT$_2$R for short). pWZL-βArrestin2-ω-IRES-Hygro plasmid is denoted as pWZL-βArrestin2 for short. Sequence integrity of each plasmid was verified by sequence analysis at StemCore Laboratories (Ottawa, ON, Canada).

The two retroviral plasmid constructs were introduced separately into Phoenix retroviral packaging cells (generous gift from Dr. Alan Mak, Queen's University) by a standard calcium phosphate method

followed 12 h later by sodium butyrate addition (10 mM). The culture medium (DMEM + 10% FBS) was replaced after another 12 h with fresh complete media (DMEM + 10% FBS + 1% penicillin/streptomycin) to harvest retroviruses released in the medium. Subsequently, C2C12 myofibroblasts (American Type Culture Collection, Manassas, VA) at ~70% confluence in 10-cm tissue culture dishes were first transduced with the βarrestin2-ω filtered viral medium (0.45 μm; Millex; Millipore, Billerica, MA) together with 4 μg/ml of Polybrene (Sigma-Aldrich). The retroviral transduction process was repeated twice at 6-h intervals to increase transduction efficiency. After transduction, cells were washed with 1× PBS and cultured in complete media for 24 h, before antibiotic selection with Hygromycin B (HyClone, Logan, UT) at initially 500 μg/ml for 1 week then tapered to 100 μg/ml. Hygromycin-resistant cells were then transduced with retroviruses expressing the $CysLT_2R$-α-fragment of β-galactosidase using the same experimental protocols. C2C12 cells transduced with both constructs (C2C12-hCysLT$_2$R-βArr for short) were then subjected to single-cell colony selection by serial dilution.

YFP fluorescence, combined with Hygromycin resistance, was used to verify expression of both constructs. Coverslips (12-mm, no. 1; Thermo Fisher Scientific) were placed in 24-well tissue culture plates and coated with 100 μl of fibronectin (Athena Enzyme Systems, Baltimore, MD). C2C12-hCysLT$_2$R-β-arrestin cells ($4–5 \times 10^4$/coverslip) were grown overnight in a 37°C incubator with 5% CO_2 in complete media. The next day, cells were washed with 1× PBS and fixed in fresh ice-cold paraformaldehyde (2%; Thermo Fisher Scientific) for 15 min before mounting with Mowiol (Merck Biosciences Ltd., Beeston, Nottingham, UK) onto slides for microscope (DMIRB; Leica, Wetzlar, Germany) viewing. The YFP signal was observed with a Green filter (515–560 nm) and analyzed with OpenLab 2 (Improvision, Lexington, MA) software for Mac. Fluorescence intensity of C2C12-hCysLT$_2$R-βArr cells was monitored as passage number increased. All assay results were produced with cells between passages 9 and 25 as signal intensity decreased after 30 passages.

To examine expression from the two constructs in C2C12 cells, total RNA was extracted with TRI reagent (Sigma-Aldrich). RNA quality was checked with an Agilent 2100 Bioanalyzer (Agilent Technologies, Santa Clara, CA) using RNA Nano chips before conducting reverse transcription PCR. cDNA was synthesized with an iScript kit (Bio-Rad Laboratories, Hercules, CA) according to the manufacturer's protocols. Oligonucleotide primers designed to anneal and amplify the junction regions of the fusion proteins were then used to verify viral transduction efficacy. Relative expression level of the two fusion proteins was assessed by quantitative PCR with the same primer sets (Table 1), normalized to GAPDH gene expression. quantitative PCR was conducted in triplicate for each gene of interest with iTaq Fast SYBR Green Supermix with ROX (Bio-Rad) kits, according to the manufacturer's protocol.

β-Galactosidase–β-Arrestin Assay. C2C12-hCysLT$_2$R-βArr cells were plated in white opaque-bottomed 96-well tissue culture plates (Corning Life Sciences, Lowell, MA) at 2.5×10^4 cells/well the night before assay, with 150 μl of complete medium. For dose response stimulation, before assay, various concentrations of stimulus in DMEM were prepared in a separate 96-well plate (stimulus plate), allowing for uniform and rapid initiation of the assays. Complete medium was then removed carefully, and 50 μl of the stimulation media was placed in each well also using a multipipette (Eppendorf). Cells were kept in the stimulation media for 1 h at 37°C before addition of Tropix Gal-Screen (50 μl; Applied Biosystems, Foster City, CA) reagent mix to each well. The Gal-Screen reagent was mixed at a substrate-buffer ratio 1:25 (v/v; manufacturer protocol), and allowed to incubate for an additional 1 h at 28°C before recording luminescence in a plate reader (FluoStar Optima; Thermo Fisher Scientific). For time-course assays, cells were stimulated up to 100 min, at 10-min intervals, with various leukotrienes in 100 μl of DMEM before addition of 100 μl of Tropix Gal-Screen reagent mix for the 1-h incubation. In total, nine different time course assays were conducted, corresponding to three different stimuli at three concentrations each. The concentrations chosen were 3× EC_{50}, 1× EC_{50}, and 1/3 EC_{50}.

Modeling and Analysis of β-Galactosidase Complementation Dynamics. The modeling was performed using the Berkeley Madonna software package (version 8.0.4; Berkeley Madonna, Berkeley, CA). Time course data were imported for $NMLTC_4$, LTD_4, and LTE_4. GPCR activation was monitored with the β-galactosidase–β-arrestin assay based on the method of von Degenfeld et al. (2007). The signal in this assay requires the receptor to be phosphorylated and to interact with β-arrestin-2. The receptor is engineered to have the α* fragment of β-galactosidase incorporated at its C terminus, whereas β-arrestin-2 is engineered to have the ω domain of β-galactosidase incorporated at its C terminus. As shown by Nichtl et al. (1998) the α and ω domains initially form a monomer that then dimerizes, after which two dimers form a tetramer to comprise the fully active β-galactosidase. Thus, in this model, the agonist, a, interacts with the engineered receptor r to form the ar complex. This then interacts with the engineered β-arrestin-2, b, to form the arb monomeric agonist–receptor–β-arrestin complex. The monomers eventually associate to form the dimer $(arb)_2$ and the corresponding tetramer $(arb)_4$.

$$a + r \underset{j_1}{\overset{k_1}{\rightleftharpoons}} ar + b \underset{j_2}{\overset{k_2}{\rightleftharpoons}} arb \underset{j_3}{\overset{k_3}{\rightleftharpoons}} (arb)_2 \underset{j_4}{\overset{k_4}{\rightleftharpoons}} (arb)_4$$

All on rate constants are denoted by k, whereas the off rate constants are denoted by j. The k_1 and j_1 values are determined exclusively by the dynamics of the agonist receptor interactions. The k_2 and perhaps j_2 values for the second step will depend on the phosphorylation state of the ligand-receptor complex. Rate constants for the last two steps of the mechanism, generation of dimer (k_3 and j_3) and the functional tetramer (k_4 and j_4), should reflect intrinsic association properties of β-galactosidase and be independent of agonist used. The rate equation for each species is shown below.

$$\frac{d[a]}{dt} = j_1[ar] - k_1[a][r]$$

$$\frac{d[r]}{dt} = j_1[ar] - k_1[a][r]$$

$$\frac{d[ar]}{dt} = k_1[a][r] + j_2[arb] - j_1[ar] - k_2[ar][b]$$

$$\frac{d[b]}{dt} = j_2[arb] - k_2[ar][b]$$

$$\frac{d[arb]}{dt} = k_2[ar][b] + j_3[(arb)_2] - j_2[arb] - k_3[arb]^2$$

TABLE 1
Primers

Junction Region	Forward Primer	Reverse Primer	Band Size
			base pairs
hCysLT2R-YFP	5′-TCAGAAAAGGCCATCCACAGA-3′	5′-AACTTGTGGCCGTTTACGTCG-3′	168
YFP-α*	5′-AACGAGAAGCGCGATCACA-3′	5′-ACGTGCTGCAAGGCGATTA-3′	158
β-Arr-ω	5′-TGTTTGAGGACTTTGCCCG-3′	5′-TTCAGGCTGCGCAACTGTT-3′	111
GAPDH	5′-CTGGAGAAACCTGCCAAGTA-3′	5′-TGTTGCTGTAGCCGTATTCA-3′	125

$$\frac{d[(arb)_2]}{dt} = k_3[arb]^2 + j_4[(arb)_4] - j_3[(arb)_2] - k_4[(arb)_2]^2$$

$$\frac{d[(arb)_4]}{dt} = k_4[(arb)_2]^2 - j_4[(arb)_4]$$

The modeling yielded time courses of the concentrations of all species of the model. The time course data of β-galactosidase for the three stimulators, LTD$_4$, LTE$_4$, and NMLTC$_4$, were fit simultaneously.

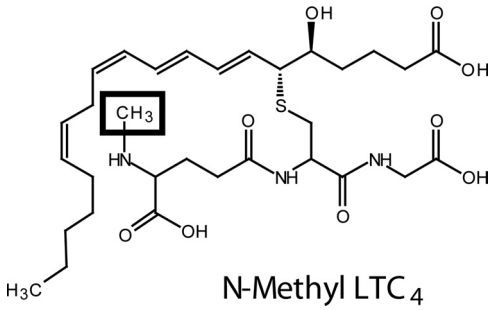

Fig. 1. Structure of NMLTC$_4$. NMLTC$_4$ is not a substrate for γ-glutamyl transpeptidase; therefore, the conversion of NMLTC$_4$ to LTD$_4$ does not occur.

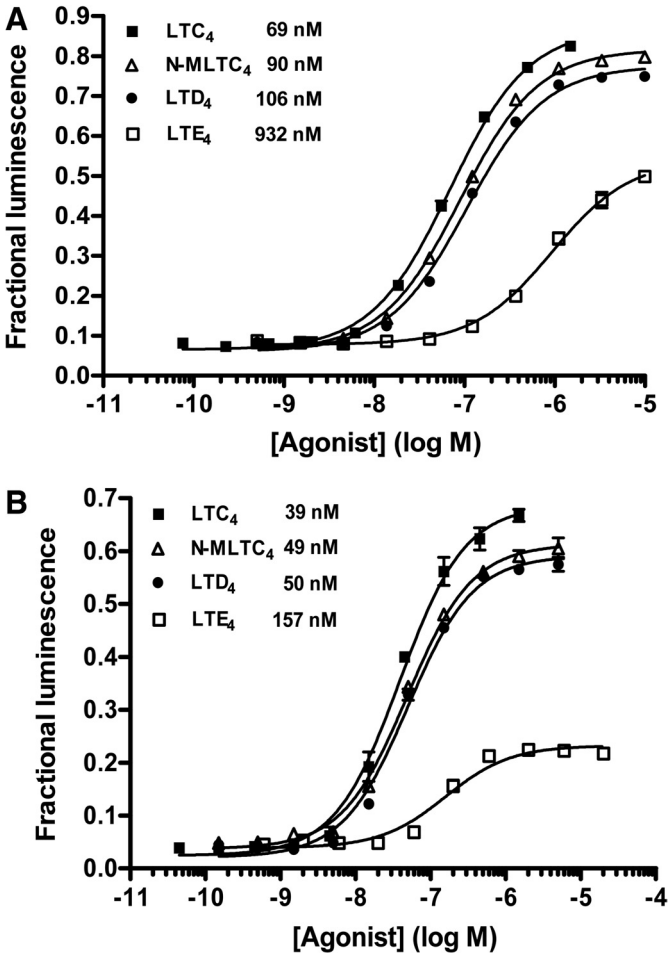

Fig. 2. NMLTC$_4$ is a full and potent agonist at the human (A) and mouse (B) CysLT$_2$ receptors. The fractional luminescence responses to LTC$_4$, LTD$_4$, LTE$_4$, and NMLTC$_4$ are plotted as a function of their concentration. Sigmoidal curves were obtained by plotting the fractional luminescence at each agonist concentration and analyzed using a modified version of the Levenberg-Marquardt four-parameter curve-fitting algorithm to determine the EC$_{50}$ values. Averages of duplicates for each sample are shown (with error bars).

TABLE 2
Potency and efficacy of leukotrienes at CysLT$_2$ receptors
EC$_{50}$ values are presented as mean ± S.E.M.

	Mouse CysLT$_2$ Receptor Aequorin Assay			Human CysLT$_2$ Receptor					
				Aequorin Assay			β-Arrestin Assay		
	Potency EC$_{50}$ (n = 3)	Pctg of Max Efficacy (Avg, n = 3)	Fold Diff EC$_{50}$ Agonist/EC$_{50}$ LTC$_4$	Potency EC$_{50}$ (n = 3)	Pctg of Max Efficacy (Avg, n = 3)	Fold Diff EC$_{50}$ Agonist/EC$_{50}$ LTC$_4$	Potency EC$_{50}$ (n = 6–8)	Pctg of Max Efficacy (Avg, n = 6–8)	Fold Diff EC$_{50}$ Agonist/EC$_{50}$ LTC$_4$
	nM	*% @ μM*		*nM*	*% @ μM*		*nM*	*% @ μM*	
LTC$_4$	38.6 ± 6.1	100 @ 1.5	1	94.6 ± 19.9	100 @ 1	1	54.4 ± 9.6	100 @ 0.8	1
NMLTC$_4$	46.1 ± 8.7	89 @ 1.5	1.2	122.3 ± 27.1	98 @ 3	1.3	8.7 ± 4.5	90 @ 0.8	0.16
LTD$_4$	49.2 ± 12.6	85 @ 1.5	1.3	144.9 ± 66.1	89 @ 3	1.5	34.7 ± 5.7	90 @ 0.9	0.64
LTE$_4$[a]	146 ± 16.7	29 @ 1.5	3.8	1208 ± 554.2	45 @ 10	12.8			

Pctg, percentage; Max, maximal; Diff, difference; Avg, average.
[a] Partial agonist.

Separate on and off rate constants for steps 1 and 2 were optimized independently for each agonist, whereas the rate constants for dimer and tetramer formation were the same for all agonists, because these steps should be independent of the identity of the agonist. In addition, a common scale factor for converting tetramer concentration to luminescence output was used. The fit of the model to the experimental data optimized by nonlinear regression using the simplex algorithm with on and off rate constants and the scale factor as best fit parameters (Table 5).

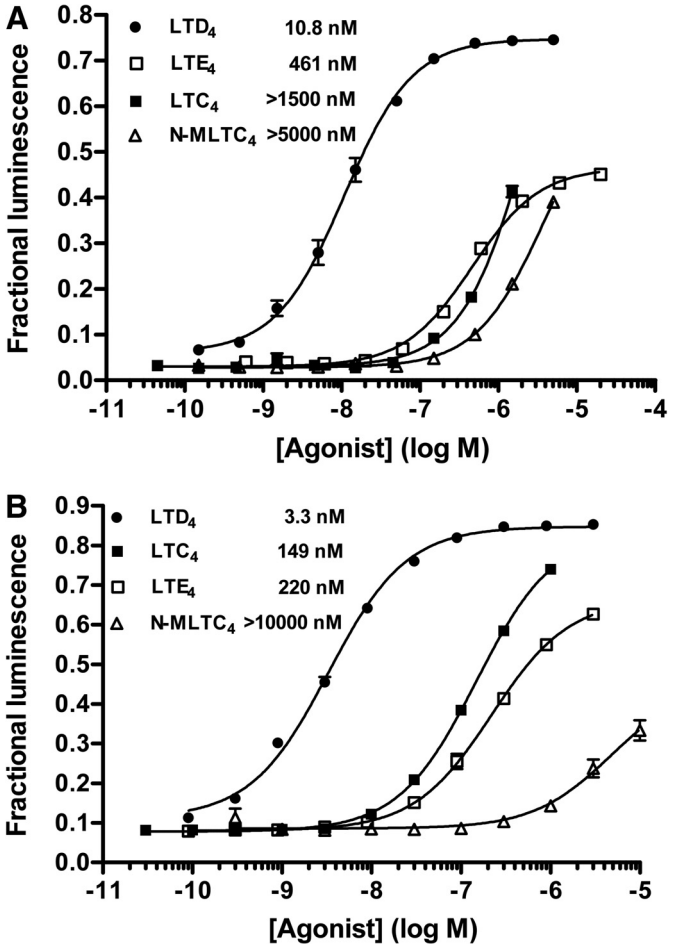

Fig. 3. $NMLTC_4$ is a very weak partial agonist at the human (A) and mouse (B) $CysLT_1$ receptors. The fractional luminescence responses to LTC_4, LTD_4, LTE_4, and $NMLTC_4$ are plotted as a function of their concentration. Sigmoidal curves were obtained by plotting the fractional luminescence at each agonist concentration and analyzed using a modified version of the Levenberg-Marquardt four-parameter curve fitting algorithm to determine the EC_{50} values. Averages of duplicates for each sample are shown (with error bars).

Vascular Ear Permeability Assay. This protocol is based on that reported by Hui et al. (2004). In short, mice were anesthetized intraperitoneally with ketamine/xylazine (0.1 ml per 10 g body weight; from 100 and 20 mg/ml stocks of ketamine (Vetalar; Boehringer Ingelheim Vetmedica, Inc., St. Joseph, MO) and xylazine (Rompun; Bayer AG, Leverkusen, Germany), respectively). Mice received 200 μl of 2% Evans Blue dye in 1× PBS via tail vein injection. Immediately thereafter, the right ear was injected intradermally with 5 ng of $NMLTC_4$ in 10 μl of saline containing 0.5% ethanol vehicle, whereas the left ear was injected with vehicle control. Animals were euthanized 15 min later. A 6-mm ear biopsy was removed and soaked in formamide (750 μl) overnight (~18 h) at 55°C, and absorbance of the extracted Evans Blue dye was measured at 610 nm with a spectrophotometer (DU-600; Beckman Coulter). Results were averaged for each experimental group and the relative increase was calculated by comparing ears injected with $NMLTC_4$ with ears injected with vehicle. T-tests were conducted with Graph-Pad Prism software using "two-tail, unpaired" conditions.

Results

$NMLTC_4$ Acts as a Full Agonist for both Human and Mouse $CysLT_2$ Receptors in an Aequorin Assay. $NMLTC_4$ was first synthesized and pharmacologically characterized by Baker et al. (1990). It was shown to be an LTC_4-mimetic that was stable and was not a substrate for γ-glutamyl transpeptidase and thus could not be converted to LTD_4 (Fig. 1), as occurs rapidly in vivo and in in vitro tissue and cell preparations. $NMLTC_4$ caused the contraction of guinea pig tracheal smooth muscle and was equipotent to LTC_4. The response to $NMLTC_4$ was not affected by either pretreatment with acivicin, an inhibitor of γ-glutamyl transpeptidase, or by addition of the $CysLT_1$ receptor antagonists zafirlukast (ICI 204219) (Baker et al., 1990) or *R*(−)-3-((3-(2-(7-chloro-2-quinolinyl)ethenyl)phenyl)(3-(dimethylamino)-3-oxo-propyl)thio)methyl) thio)propanoic acid (MK679).

To test the CysLT receptor subtype selectivity of $NMLTC_4$, the $CysLT_1$ or $CysLT_2$ receptor cDNAs from human or mouse were introduced into a heterologous expression system with an aequorin-based functional assay for calcium-coupled GPCRs (Ungrin et al., 1999). HEK cells were stimulated with various concentrations of leukotrienes, including LTC_4, LTD_4, LTE_4, and $NMLTC_4$. At the human or mouse $CysLT_2$ receptor, LTC_4 was the most potent agonist followed closely by $NMLTC_4$ and LTD_4. LTE_4 was a weak partial agonist at both receptors (Fig. 2 and Table 2). Thus, in this aequorin assay system, $NMLTC_4$ behaves as a full agonist at $CysLT_2$ receptor.

TABLE 3
Potency and efficacy of leukotrienes at $CysLT_1$ receptors
EC_{50} values are presented as mean ± S.E.M.

	$CysLT_1$ Receptor					
	Mouse			Human		
	Potency EC_{50} (n = 3)	Pctg of Max Efficacy (Avg, n = 3)	Fold Diff EC_{50} Agonist/EC_{50} LTD_4	Potency EC_{50} (n = 3)	Pctg of Max Efficacy (Avg, n = 3)	Fold Diff EC_{50} Agonist/EC_{50} LTD_4
	nM	*% @ μM*		*nM*	*% @ μM*	
LTD_4	5.4 ± 0.8	100 @ 0.3	1	11.6 ± 5.5	100 @ 0.4	1
LTC_4[a]	183 ± 27.8	84 @ 1	34	1483 ± 516	62 @ 1	128
LTE_4[a]	231 ± 1.3	73 @ 3	43	391 ± 48.7	66 @ 5	34
$NMLTC_4$[a]	≥3000	28 @ 10	≥ 556	≥2000	60 @ 40	≥172

Pctg, percentage; Max, maximal; Diff, difference; Avg, average.
[a] Partial agonist.

At the CysLT$_1$ receptors, NMLTC$_4$ was a very weak partial agonist (Fig. 3 and Table 3), ≥172- and ≥556-fold less potent than LTD$_4$ for human and mouse CysLT$_1$ receptor, respectively. LTC$_4$ and LTE$_4$ were weak agonists for both CysLT$_1$ receptor homologs. The rank orders of NMLTC$_4$ and the cysLTs for the various receptors are shown in Table 4. Thus, NMLTC$_4$ is almost as potent as LTC$_4$ at the CysLT$_2$ receptors and is the least efficacious agonist at the CysLT$_1$ receptors, far less active than any other cysLT tested. LTE$_4$ is a weak partial agonist for both receptor subtypes in both species tested in the aequorin assay.

NMLTC$_4$ Is a Full Agonist for Human CysLT$_2$ Receptor in a β-Galactosidase- β-Arrestin Assay. Because of the inherent promiscuous nature of secondary messengers such as intracellular calcium (von Degenfeld et al., 2007), a β-galactosidase complementation assay involving β-arrestin-2 binding was developed for the hCysLT$_2$ receptor (Fig. 4). Interactions of the hCysLT$_2$ receptor with β-arrestin-2 have not previously been assessed. This assay takes advantage of homologous desensitization to indirectly assess the activation of the hCysLT$_2$ receptor. Results from this assay add a layer of specificity, either downstream or parallel to the Ca^{2+} signaling, for hCysLT$_2$ receptor signaling. C2C12 myofibroblasts transduced with retroviral constructs expressing both hCysLT$_2$ receptor and β-arrestin-2 were selected based on fluorescence intensity from the YFP fusion of the receptor and by Hygromycin resistance. Quantitative real-time PCR was conducted after the first round of transduction, with pWZL-βarrestin2, to determine the

TABLE 4
Rank order of agonist potencies at the CysLT receptors

	Aequorin Assays	β-Arrestin Assay
hCysLT$_2$R	LTC$_4$ ≥ NMLTC$_4$ ≥ LTD$_4$ ≫ LTE$_4$	NMLTC$_4$ ≥ LTC$_4$, LTD$_4$ ≫ LTE$_4$
mCysLT$_2$R	LTC$_4$ ≥ NMLTC$_4$ ≥ LTD$_4$ > LTE$_4$	
hCysLT$_1$R	LTD$_4$ ≫ LTE$_4$ ≫ LTC$_4$ > NMLTC$_4$	
mCysLT$_1$R	LTD$_4$ ≫ LTC$_4$ > LTE$_4$ ≫ NMLTC$_4$	

h, human; m, mouse.

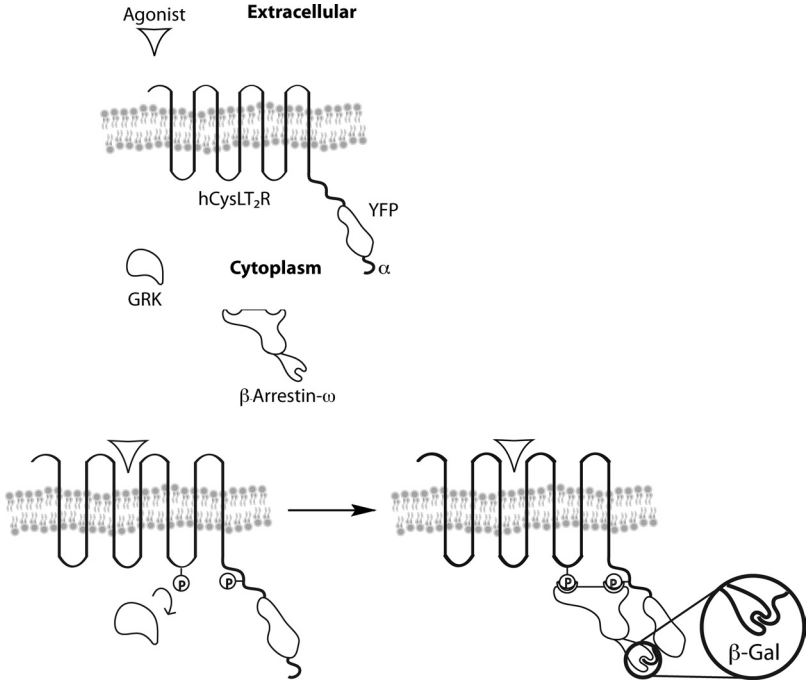

Fig. 4. Depiction of β-galactosidase–β-arrestin complementation assay. Top, various signaling components in assay system. Bottom, prolonged cysLT agonist stimulation of the hCysLT$_2$ receptor leads to receptor phosphorylation by G protein receptor kinases (GRKs) with subsequent recruitment of β-arrestin, which allows for complementation of the two β-galactosidase fragments α and ω for enzyme activity assay.

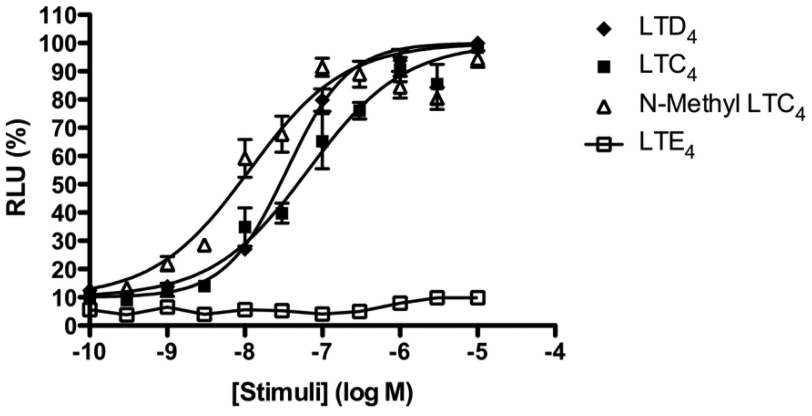

Fig. 5. NMLTC$_4$ is a full and potent agonist at the human CysLT$_2$ receptor in the β-galactosidase–β-arrestin assay. The fractional luminescence response to LTC$_4$, LTD$_4$, LTE$_4$, and NMLTC$_4$ were plotted as a function of their concentration. Results were analyzed with Prism 4 (GraphPad Software, San Diego, CA), with "dose-response curve" settings, upper constrain set to "equal to 100," and bottom constrain set to "less than 10." Average of duplicate assays with multiple cell preparations (n = 6–8) for each sample are shown.

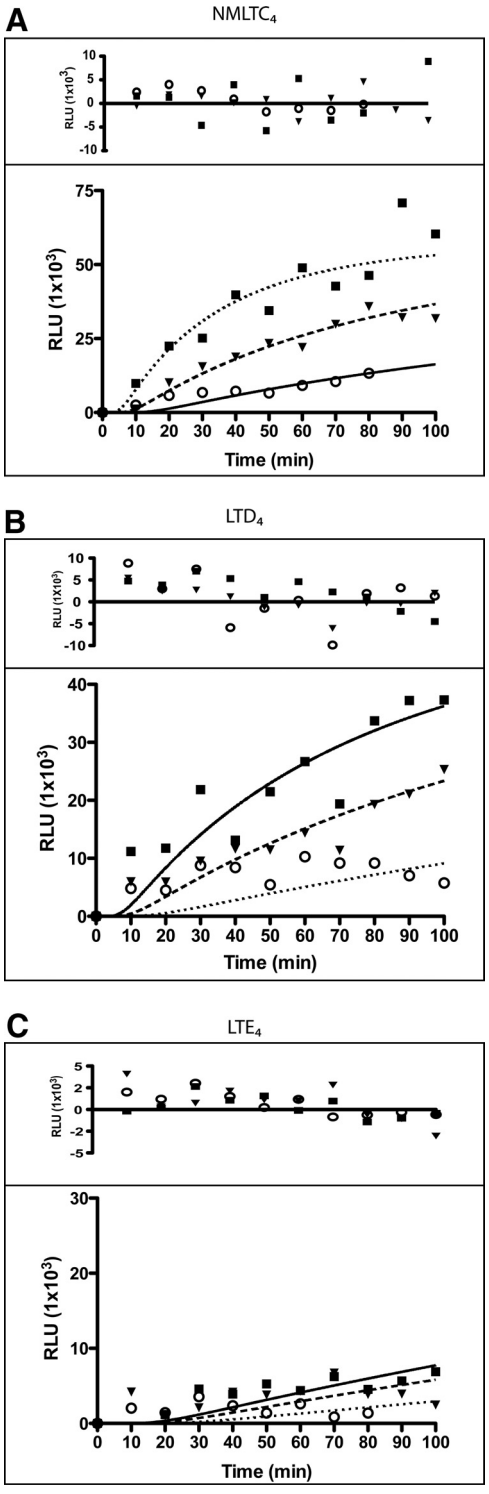

Fig. 6. Computer simulation data using β-galactosidase mechanism to model the β-arrestin assay dynamics in silico. The output of tetramer concentration, from Berkeley Madonna, converted to luminescence readout by the scale factor was overlaid with experimental results in GraphPad Prism. A, the experimental data of $NMLTC_4$, depicted by ■, ▼, and ○, as concentrations of 3× EC_{50}, 1× EC_{50}, and 1/3x EC_{50}, respectively. The modeled data are depicted by solid, dashed, and dotted lines at the three respective concentrations. The same legend is used in B and C, as overlays of experimental and computer-modeled data for LTD_4 and LTE_4, respectively. The corresponding residual plots, using the same time axis as the overlay, are shown above the individual graphs.

colony with the highest expression of β-arrestin-2 (colony G, data not shown). The colony G cells were used in the second round of transduction, with pMFG-hCysLT$_2$R to establish doubly transduced cells. After completion of both rounds of transduction, single clone isolates were then established, and one clonal expansion (colony 2) was used for all data collection based on the YFP signal intensity, referred to hereafter as C2C12-hCysLT$_2$R-βArr. YFP signal was observed to decrease over time in culture, so cells were periodically replaced with low-passage cell stocks maintained in liquid nitrogen.

C2C12-hCysLT$_2$R-βArr cells were stimulated with various concentrations of leukotrienes, as well as $NMLTC_4$. The results indicate that $NMLTC_4$ is somewhat more potent than both LTC_4 and LTD_4 in physiologically relevant concentrations (Fig. 5, Table 2). LTE_4 in this assay hardly elicits any response above baseline, even with concentrations up to 10^{-5} M (Fig. 5). LTB_4, a non-cysLT product, was devoid of agonist activity, as were nucleotides (ATP, ADP, UDP and UTP; data not shown).

In time-course assays with constant concentrations of leukotrienes, $NMLTC_4$ and LTD_4 display time-dependent profiles (Fig. 6). Consistent with dose-response curves, LTE_4 did not evoke significant β-galactosidase signal output even with stimulation periods up to 100 min with micromolar concentrations.

Modeling Simulation of CysLT$_2$R–β-Arrestin–β-Galactosidase Complementation in Time-Course Assays. The β-galactosidase time-course data for LTD_4, LTE_4, and $NMLTC_4$, each at concentrations of 1/3 EC_{50}, EC_{50}, and 3× EC_{50}, are shown in Fig. 6. The lines in Fig. 6 are regression lines obtained through modeling. $NMLTC_4$ and LTD_4 gave much higher levels of β-galactosidase activity (as measured by luminescence), and their time courses were also clearly dose-dependent. In addition, the model simulated the experimental results reasonably well, especially with $NMLTC_4$ and LTD_4. The fit with LTE_4 was not as good, indicating that the signal output from the assay is nearing the detection limit. The simulation yielded rate constants for each of the steps in the model, as listed in Table 5. Agonist dose responses at 60 min were simulated to determine whether the model could yield consistent EC_{50} values as with experimental data (shown in Fig. 5). The simulated β-galactosidase values at 60 min were fitted to the equation $Y = (Y_{max} \times [\text{Agonist}])/(EC_{50} + [\text{Agonist}])$, where Y is the simulated β-ga-

TABLE 5
Rate constants fitted to experimental data in silico by fixing the k_3, j_3, k_4, and j_4 values between data sets

$$a+r \underset{j_1}{\overset{k_1}{\rightleftharpoons}} ar+b \underset{j_2}{\overset{k_2}{\rightleftharpoons}} arb \underset{j_3}{\overset{k_3}{\rightleftharpoons}} (arb)_2 \underset{j_4}{\overset{k_4}{\rightleftharpoons}} (arb)_4$$

	$NMLTC_4$	LTE_4	LTD_4
k_1 ($M^{-1} \cdot s^{-1}$)	1.06×10^6	1.06×10^4	8.28×10^5
j_1 (s^{-1})	9.51×10^{-2}	9.47×10^{-3}	1.12×10^{-1}
K_{d1} (nM)	89.76	891.9	135.0
k_2* ($M^{-1} \cdot s^{-1}$)	4.33×10^5	7.57×10^{3}*	1.06×10^6
j_2 (s^{-1})	10^{-4}	1.41×10^{-3}	7.39×10^{-2}
K_{d2} (nM)	0.2	186.2	69.8
k_3 ($M^{-1} \cdot s^{-1}$)	2.72×10^7	2.72×10^7	2.72×10^7
j_3 (s^{-1})	1.04×10^{-5}	1.04×10^{-5}	1.04×10^{-5}
K_{d3} (M)	3.82×10^{-13}	3.82×10^{-13}	3.82×10^{-13}
k_4 ($M^{-1} \cdot s^{-1}$)	2.98×10^7	2.98×10^7	2.98×10^7
j_4 (s^{-1})	2.83×10^{-5}	2.83×10^{-5}	2.83×10^{-5}
K_{d4} (M)	9.52×10^{-13}	9.52×10^{-13}	9.52×10^{-13}
Scale factor	58,801.8	58,801.8	58,801.8

lactosidase activity. The simulations fit the experimental data very well and yield estimated EC_{50} values of 9.9, 54.8, and 2268 nM for $NMLTC_4$, LTD_4, and LTE_4, respectively. These compared favorably with the experimentally measured β-galactosidase–β-arrestin values of 8.5 and 36 nM for $NMLTC_4$ and LTD_4, respectively. LTE_4 was previously determined to have an EC_{50} of 2300 nM by Ca^{2+} functional assay (Heise et al., 2000). The similarity between the "simulated" EC_{50} values and the actual experimental results lend to the added confidence toward the computational modeling and the equilibrium rate equations describing each interaction.

The model indicates that the dynamics of the β-galactosidase response in this assay system is determined primarily by the on rate constant at step two (k_2). The k_2 values for $NMLTC_4$ and LTD_4 are 4.33×10^5 $M^{-1} \cdot s^{-1}$ and 1.06×10^6 $M^{-1} \cdot s^{-1}$, respectively, whereas the k_2 value for LTE_4 is remarkably smaller at 7.57×10^3 $M^{-1} \cdot s^{-1}$. This is worth noting as it might point toward a slower phosphorylation step by G protein receptor kinases after receptor activation, which could not be measured directly in the assay conditions. It is important to point out that this computer modeling is not a mechanistic interpretation but rather provides a rationale for the low results for LTE_4 in the β-arrestin assay. Each of the eight parameters was independently adjusted by 0.01% to determine the effect on the computed values of output (relative light units). This sensitivity analysis is tabulated in the Supplemental Data (Supplemental Table 1). In general, the final output was most sensitive to the on rate constant for the β-arrestin binding (k_2) for all compounds at all concentrations. The result of the sensitivity analysis hints that k_2 plays a pivotal role in determining the final output of the assay.

$NMLTC_4$ Is a Selective Agonist for the hCysLT$_2$ Receptor In Vivo. $NMLTC_4$ was injected into the ears of transgenic mice overexpressing the hCysLT$_2$ receptor in vascular endothelial cells (TG-EC) (Hui et al., 2004) and in the CysLT$_2$R knockout (KO) mice (Moos et al., 2008). $NMLTC_4$ elicited a large, statistically significant increase in Evans Blue dye leakage in the TG-EC mice compared with vehicle-treated ears (Fig. 7). In KO mice, on the other hand, $NMLTC_4$ did not increase vascular leakage, indicating a CysLT$_2$ receptor-mediated leakage and selectivity of the agonist in vivo.

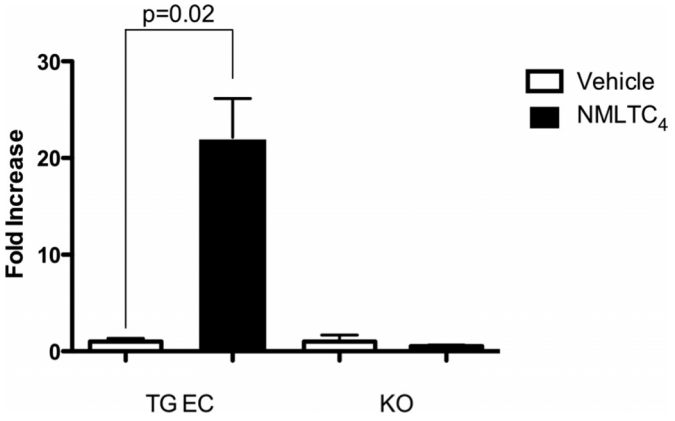

Fig. 7. $NMLTC_4$ is a potent selective agonist at the CysLT$_2$ receptor in vivo. TG-EC mice showed a 22-fold increase in vascular leakage upon $NMLTC_4$ administration compared with vehicle control (set to 1.0) as measured by optical density at 610 nm. Mice lacking the CysLT$_2$ receptor showed no statistically significant response to $NMLTC_4$ compared with vehicle-treated ears. Average absorbencies were 0.012 ± 0.01 (TG-EC, vehicle; $n = 8$), 0.26 ± 0.13 (TG-EC, $NMLTC_4$; $n = 8$), 0.063 ± 0.07 (KO, vehicle; $n = 3$), and 0.034 ± 0.01 (KO, $NMLTC_4$; $n = 3$).

Discussion

Here we demonstrate that $NMLTC_4$ (Fig. 1) is a CysLT$_2$-receptor-subtype–selective, potent agonist using two distinct assays that target Ca^{2+} signaling and downstream β-arrestin 2 binding to the phosphorylated receptor. The β-arrestin assay offers distinct specificity and low background activation by monitoring a homologous desensitization pathway and this is the first time a specific interaction of the CysLT$_2$ receptor with β-arrestin is demonstrated. Growing evidence suggests an inherent bias of GPCR signaling toward either trimeric G-protein or β-arrestin 2, depending on the receptor in question, as well as the agonist (Violin and Lefkowitz, 2007). The data obtained in the present study with these assays enhances our knowledge of the understudied CysLT$_2$ receptor signaling pathways.

$NMLTC_4$ should be a very useful tool to selectively activate the CysLT$_2$ receptor, both in vitro and in vivo, without affecting the CysLT$_1$ receptor, and we have demonstrated its efficacy in vivo in an ear vascular permeability assay. $NMLTC_4$ has been tested in the bullfrog, looking at cardiovascular effects (Sun and Herman, 1995) and lung contractions (Herman et al., 1995) before discernment of its subtype selectivity at the recombinant CysLT$_2$ versus CysLT$_1$ receptors as demonstrated in this present study. The role that the CysLT$_2$ receptor plays in normal and diseased states is being examined. Its distribution in the human heart and vasculature, adrenal gland, immune cells, brain, and other tissues (Heise et al., 2000; Nothacker et al., 2000; Kamohara et al., 2001; Evans, 2002) suggests that the CysLT$_2$ receptor is potentially involved in both physiological and pathophysiological processes. In animal models, we have demonstrated that transgenic expression of the hCysLT$_2$ receptor in vascular endothelium predisposes to heightened myocardial ischemia-reperfusion injury and increased vascular permeability in certain vascular beds (Jiang et al., 2008; Moos et al., 2008). The CysLT$_2$ receptor has been implicated in allergic and inflammatory diseases such as asthma, rhinitis, and sinusitis (Pillai et al., 2004; Steinke and Borish, 2004), as well as in cerebral inflammation and edema (Di Gennaro et al., 2004). Leukotrienes are likely to play an important role in the progression of pulmonary hypertension (Jones et al., 2004) and in cardiovascular disease (Helgadottir et al., 2004; Funk, 2005). Probing the role that CysLT$_2$ receptor plays in these disease processes may now be approached using the selective agonist $NMLTC_4$.

Of the CysLTs, especially pertaining to LTE_4, there was a differential response in the two assays; in the aequorin assay LTE_4 behaved as a partial agonist but was unable to elicit a signal above baseline in the β-arrestin assay. Through computer modeling, a possible explanation of the observation is that LTE_4 activates Ca^{2+} signaling through G_q but is unable to induce a tight enough association between the ligand-bound receptor and β-arrestin, possibly as a result of weak receptor phosphorylation induced by this cysLT. The biased nature of agonist signaling through one receptor (Violin and Lefkowitz, 2007) is not without precedence; the μ-opioid receptor (Keith et al., 1996) is one well characterized example. These results with LTE_4 are significant given the recent de-

termination of a (putative) LTE_4-selective receptor ($CysLT_E$) and that LTE_4 can apparently act via non-GPCR pathways (e.g., peroxisome proliferator-activated receptor-γ) (Paruchuri et al., 2008). LTE_4 signaling via the $hCysLT_2$ receptor apparently displays preference toward trimeric G-protein signaling rather than via β-arrestin 2 pathways, as evidenced by the calcium activity but lack of β-arrestin 2 association. This signaling bias may afford a novel means to study the CysLT receptors.

In summary, we have shown that $NMLTC_4$ is a potent subtype-selective agonist for the $CysLT_2$ receptor both in vitro and in vivo. Importantly, it can be used as a selective tool together with the recently described (Wunder et al., 2010) first selective $CysLT_2$ receptor antagonist, HAMI3379, to identify some of the physiological and pathophysiological roles that the $CysLT_2$ receptor plays in tissues and cells in which it has been identified and in various disease states.

Acknowledgments

We thank Mark Daubaras, Luke Zheng, and Tim St. Amand for assistance with the β-galactosidase assay, as well as Jalna Meens and Laurel Ballantyne for assistance with the vascular permeability assay. Yves Gareau and Jeff Johnson (Cayman Chemical Company) are acknowledged for the synthesis of $NMLTC_4$ used in the studies, and Bo Cheyne and Viviane Martin for work on the aequorin assays. We thank Jilly F. Evans for helpful discussions on this project.

Authorship Contributions

Participated in research design: Yan, Stocco, Nesheim, Abramovitz, and Funk.

Conducted experiments: Yan, Stocco, Sawyer, and Nesheim.

Performed data analysis: Yan, Stocco, and Nesheim.

Wrote or contributed to the writing of the manuscript: Yan, Stocco, Nesheim, Abramovitz, and Funk.

References

Aharony D, Dobson PT, and Krell RD (1985) In vitro metabolism of [^{3}H]peptide leukotrienes in human and ferret lung: a comparison with the guinea pig. *Biochem Biophys Res Commun* **131:**892–898.

Baker SR, Boot JR, Gooderham R, O'Brien A, Thomas KH, Ward M, and Woodhouse S (1990) The pharmacology of N-methyl LTC4; a metabolically stable LTC4-mimetic. *Prostaglandins* **40:**445–461.

Coleman RA, Eglen RM, Jones RL, Narumiya S, Shimizu T, Smith WL, Dahlén SE, Drazen JM, Gardiner PJ, Jackson WT, et al. (1995) Prostanoid and leukotriene receptors: a progress report from the IUPHAR working parties on classification and nomenclature. *Adv Prostaglandin Thromboxane Leukot Res* **23:**283–285.

Di Gennaro A, Carnini C, Buccellati C, Ballerio R, Zarini S, Fumagalli F, Viappiani S, Librizzi L, Hernandez A, Murphy RC, et al. (2004) Cysteinyl-leukotrienes receptor activation in brain inflammatory reactions and cerebral edema formation: a role for transcellular biosynthesis of cysteinyl-leukotrienes. *FASEB J* **18:**842–844.

Evans JF (2002) Cysteinyl leukotriene receptors. *Prostaglandins Other Lipid Mediat* **68–69:**587–597.

Funk CD (2001) Prostaglandins and leukotrienes: advances in eicosanoid biology. *Science* **294:**1871–1875.

Funk CD (2005) Leukotriene modifiers as potential therapeutics for cardiovascular disease. *Nat Rev Drug Discov* **4:**664–672.

Gareau Y, Zamboni R, and Wong AW (1993) Total synthesis of N-methyl LTC4- A novel methodology for the monomethylation of amines. *J Org Chem* **58:**1582–1585.

Grossman J, Ratner PH, Nathan R, Adelglass J, and deJong B (1997) Pranlukast (Ultair(TM), SB 205312, ONO-1078), an oral leukotriene receptor antagonist, relieves symptoms in patients with seasonal allergic rhinitis (SAR). *J Allerg Clin Immunol* **99:**1799.

Heise CE, O'Dowd BF, Figueroa DJ, Sawyer N, Nguyen T, Im DS, Stocco R, Bellefeuille JN, Abramovitz M, Cheng R, et al. (2000) Characterization of the human cysteinyl leukotriene 2 receptor. *J Biol Chem* **275:**30531–30536.

Herman CA, Skarda S, Romero MA, Chapunoff D, Schulmeister K, and Torres OA (1995) Leukotriene C4-stimulated contractions in bullfrog lung are affected by cold acclimation and calcium antagonists. *Prostaglandins* **49:**117–129.

Helgadottir A, Manolescu A, Thorleifsson G, Gretarsdottir S, Jonsdottir H, Thorsteinsdottir U, Samani NJ, Gudmundsson G, Grant SF, Thorgeirsson G, et al. (2004) The gene encoding 5-lipoxygenase activating protein confers risk of myocardial infarction and stroke. *Nat Genet* **36:**233–239.

Hui Y, Cheng Y, Smalera I, Jian W, Goldhahn L, Fitzgerald GA, and Funk CD (2004) Directed vascular expression of human cysteinyl leukotriene 2 receptor modulates endothelial permeability and systemic blood pressure. *Circulation* **110:**3360–3366.

Hui Y, Yang G, Galczenski H, Figueroa DJ, Austin CP, Copeland NG, Gilbert DJ, Jenkins NA, and Funk CD (2001) The murine cysteinyl leukotriene 2 (CysLT(2)) receptor—cDNA and genomic cloning, alternative splicing, and in vitro characterization. *J Biol Chem* **276:**47489–47495.

Jiang W, Hall SR, Moos MP, Cao RY, Ishii S, Ogunyankin KO, Melo LG, and Funk CD (2008) Endothelial cysteinyl leukotriene 2 receptor expression mediates myocardial ischemia-reperfusion injury. *Am J Pathol* **172:**592–602.

Jones JE, Walker JL, Song Y, Weiss N, Cardoso WV, Tuder RM, Loscalzo J, and Zhang YY (2004) Effect of 5-lipoxygenase on the development of pulmonary hypertension in rats. *Am J Physiol Heart Circ Physiol* **286:**H1775–H1784.

Kamohara M, Takasaki J, Matsumoto M, Matsumoto Si, Saito T, Soga T, Matsushime H, and Furuichi K (2001) Functional characterization of cysteinyl leukotriene CysLT(2) receptor on human coronary artery smooth muscle cells. *Biochem Biophys Res Commun* **287:**1088–1092.

Keith DE, Murray SR, Zaki PA, Chu PC, Lissin DV, Kang L, Evans CJ, and von Zastrow M (1996) Morphine activates opioid receptors without causing their rapid internalization. *J Biol Chem* **271:**19021–19024.

Labat C, Ortiz JL, Norel X, Gorenne I, Verley J, Abram TS, Cuthbert NJ, Tudhope SR, Norman P, and Gardiner P (1992) A second cysteinyl leukotriene receptor in human lung. *J Pharmacol Exp Ther* **263:**800–805.

Lynch KR, O'Neill GP, Liu Q, Im DS, Sawyer N, Metters KM, Coulombe N, Abramovitz M, Figueroa DJ, Zeng Z, et al. (1999) Characterization of the human cysteinyl leukotriene CysLT1 receptor. *Nature* **399:**789–793.

Maekawa A, Kanaoka Y, Xing W, and Austen KF (2008) Functional recognition of a distinct receptor preferential for leukotriene E4 in mice lacking the cysteinyl leukotriene 1 and 2 receptors. *Proc Natl Acad Sci USA* **105:**16695–16700.

Martin V, Sawyer N, Stocco R, Unett D, Lerner MR, Abramovitz M, and Funk CD (2001) Molecular cloning and functional. characterization of murine cysteinyl-leukotriene 1 (CysLT(1)) receptors. *Biochem Pharmacol* **62:**1193–1200.

Moos MP, Mewburn JD, Kan FW, Ishii S, Abe M, Sakimura K, Noguchi K, Shimizu T, and Funk CD (2008) Cysteinyl leukotriene 2 receptor-mediated vascular permeability via transendothelial vesicle transport. *FASEB J* **22:**4352–4362.

Nichtl A, Buchner J, Jaenicke R, Rudolph R, and Scheibel T (1998) Folding and association of beta-galactosidase. *J Mol Biol* **282:**1083–1091.

Nothacker HP, Wang Z, Zhu Y, Reinscheid RK, Lin SH, and Civelli O (2000) Molecular cloning and characterization of a second human cysteinyl leukotriene receptor: discovery of a subtype selective agonist. *Mol Pharmacol* **58:**1601–1608.

Pillai SG, Cousens DJ, Barnes AA, Buckley PT, Chiano MN, Hosking LK, Cameron LA, Fling ME, Foley JJ, Green A, et al. (2004) A coding polymorphism in the CYSLT2 receptor with reduced affinity to LTD_4 is associated with asthma. *Pharmacogenetics* **14:**627–633.

Pong SS and DeHaven RN (1983) Characterization of a leukotriene D4 receptor in guinea pig lung. *Proc Natl Acad Sci USA* **80:**7415–7419.

Paruchuri S, Jiang Y, Feng C, Francis SA, Plutzky J, and Boyce JA (2008) Leukotriene E4 activates peroxisome proliferator-activated receptor gamma and induces prostaglandin D2 generation by human mast cells. *J Biol Chem* **283:**16477–16487.

Reiss TF, Chervinsky P, Dockhorn RJ, Shingo S, Seidenberg B, and Edwards TB (1998) Montelukast, a once-daily leukotriene receptor antagonist, in the treatment of chronic asthma: a multicenter, randomized, double-blind trial. Montelukast Clinical Research Study Group. *Arch Intern Med* **158:**1213–1220.

Sarau HM, Ames RS, Chambers J, Ellis C, Elshourbagy N, Foley JJ, Schmidt DB, Muccitelli RM, Jenkins O, Murdock PR, et al. (1999) Identification, molecular cloning, expression, and characterization of a cysteinyl leukotriene receptor. *Mol Pharmacol* **56:**657–663.

Steinke JW and Borish L (2004) Leukotriene receptors in rhinitis and sinusitis. *Curr Allergy Asthma Rep* **4:**217–223.

Suissa S, Dennis R, Ernst P, Sheehy O, and Wood-Dauphinee S (1997) Effectiveness of the leukotriene receptor antagonist zafirlukast for mild-to-moderate asthma. A randomized, double-blind, placebo-controlled trial. *Ann Intern Med* **126:**177–1863.

Sun J and Herman CA (1995) Cardiovascular effects of N-methyl leukotriene C_4, a nonmetabolizable leukotriene C_4 analogue, and the antagonism of leukotriene-induced hypotension by Ro 23-3544, in the American bullfrog, Rana catesbeiana. *Can J Physiol Pharmacol* **73:**383–389.

Takasaki J, Kamohara M, Matsumoto M, Saito T, Sugimoto T, Ohishi T, Ishii H, Ota T, Nishikawa T, Kawai Y, et al. (2000) The molecular characterization and tissue distribution of the human cysteinyl leukotriene CysLT(2) receptor. *Biochem Biophys Res Commun* **274:**316–322.

Ungrin MD, Singh LM, Stocco R, Sas DE, and Abramovitz M (1999) An automated aequorin luminescence-based functional calcium assay for G-protein-coupled receptors. *Anal Biochem* **272:**34–42.

Violin JD and Lefkowitz RJ (2007) Beta-Arrestin-biased ligands at seven-transmembrane receptors. *Trends Pharmacol Sci* **28:**416–422.

von Degenfeld G, Wehrman TS, Hammer MM, and Blau HM (2007) A universal technology for monitoring G-protein-coupled receptor activation in vitro and non-invasively in live animals. *FASEB J* **21:**3819–3826.

Walch L, Norel X, Gascard JP, and Brink C (1999) Cysteinyl-leukotriene receptors in pulmonary vessels. *J Physiol Pharmacol* **50:**567–573.

Wunder F, Tinel H, Kast R, Geerts A, Becker EM, Kolkhof P, Hütter J, Ergüden J, and Härter M (2010) Pharmacological characterization of the first potent and selective antagonist at the cysteinyl leukotriene 2 (CysLT(2)) receptor. *Br J Pharmacol* **160:**399–409.

Address correspondence to: Dr. Colin D. Funk, Department of Physiology, Queen's University, 18 Stuart Street, 433 Botterell Hall, Kingston, ON K7L 3N6 Canada. E-mail: funkc@queensu.ca